IEEE Access
Multidisciplinary | Rapid Review | Open Access Journal

Received August 22, 2018, accepted September 24, 2018, date of publication October 12, 2018, date of current version November 9, 2018.

Digital Object Identifier 10.1109/ACCESS.2018.2875680

A High-Gain Transmitarray for Generating Dual-Mode OAM Beams

FAN QIN[1], (Member, IEEE), STEVEN GAO[2], (Member, IEEE), WEN-CHI CHENG[1], (Senior Member, IEEE), YI LIU[1], (Senior Member, IEEE), HAI-LIN ZHANG[1], (Member, IEEE), AND GAO WEI[3]

[1]State Key Laboratory of Integrated Services Networks, Xidian University, Xi'an 710071, China
[2]School of Engineering and Digital Arts, University of Kent, Canterbury CT2 7NT, U.K.
[3]School of Electronics and Information, Northwestern Polytechnical University, Xi'an 710072, China

Corresponding author: Fan Qin (fqin@xidain.edu.cn)

This work was supported in part by National Natural Science Foundation of China under Contract 61701362 and Contract 61671347 and in part by the 111 Project of China (B08038).

ABSTRACT This paper proposes a novel transmitarray antenna which can achieve high gain and produce dual-mode orbital angular momentum (OAM) beams in *Ku*-band. Two back-to-back wideband dual-polarized microstrip antennas are employed as the unit cells, which are connected using metalized via holes. Full 360° phase ranges can be obtained by varying the length of feeding lines in two orthogonal polarizations. Due to high isolation between the two orthogonal polarizations, dual-mode OAM beams can be formed simultaneously by tuning phase distributions in x- and y-polarizations, respectively. The approach for generating OAM beams is explained. To verify this concept, one prototype carrying 0 and +1 mode OAM beams is designed, fabricated, and measured. Experimental results demonstrate that both 0 and +1 mode OAM beams can be generated successfully, and the measured results agree well with the simulated results. Because of high directivity and focusing effects of transmitarray, the proposed +1 mode OAM beam has stable performance at a long propagation distance. The maximum gain reaches 26 and 20 dBi in 0 and +1 mode OAM beams, respectively. Meanwhile, a narrow divergence angle of ±5° is obtained in +1 mode OAM beam. Compared with other OAM antennas reported, main advantages of the proposed antenna include high gain, narrow divergence angle, low cost, planar structure, and the capability of producing dual-mode OAM beams.

INDEX TERMS Orbital angular momentum (OAM), dual-mode, high-gain, transmitarray.

I. INTRODUCTION

With the rapid development of wireless communication, it has become a major challenge to provide faster and higher data capacity with limited radio resources. As a promising technique, orbital angular momentum (OAM) is expected to potentially improve channel capacity and spectrum efficiency [1]. Compared to plane waves, OAM waves have helical phase fronts with $2\pi l$ phase shifts, where l is OAM mode which can be any positive or negative integer. When l is 0, namely 0 OAM mode, the proposed OAM waves is plane waves without phase twist [2]. Due to the orthogonality of different OAM modes of the vortex beam, it is possible to build individual channel using one mode with little interaction on other modes at the same working frequency. This property leads to the potential of transmitting high density information using mode multiplexing technique.

OAM was investigated in optical region initially. L. Allen demonstrated experimentally that electromagnetic (EM) waves can carry OAM [3]. Since then, OAM gave rise to many applications in optical domain, such as optical manipulation, optical trapping, imaging and so on [4]–[7]. In [8], an optical wireless link reached a data rate of 2.56 Tbit/s by using OAM beams. The concept of OAM was introduced in radio region as well. In 2007, Thidé *et al.* [9] first proposed that OAM can be used in lower frequency. Later, extending communications capacity using OAM beams starts a new page for OAM applications in radio frequency. The first radio frequency experiments for generating and detect-

ing OAM waves in laboratory was reported in 2011 [10]. In 2012, an OAM-based wireless connection over a distance of 442 m was demonstrated in a real-world setting, where two radio waves encoded with different OAM beams at the same frequency [11]. In further research, OAM was applied in millimeter-wave (mm-wave) domain [12]. One example is that a dual-channel 60 GHz communications using OAM beams was demonstrated [13]. In this study, a mm-wave wireless link reached 8-Gbit/s and 4-Gbit/s using different OAM modes.

As a key complement generating OAM beams, antennas play a very important role in OAM wireless system. Many antennas have been studied to generate OAM beams. Typical approaches such as spiral phase plane (SPP) and helicoidal parabolic antenna are often employed to generate OAM beams [14]–[16]. In [10], a discrete eight-step staircase phase reflector was used to create a discontinues phase shift for OAM beam generation. Using a similar approach, a helicoidal parabolic antenna was fabricated and tested [11]. But these antennas have non-planar structures, bulky sizes, heavy weight, high fabrication complexity and high cost. More importantly, it is difficult to produce dual-mode OAM beams. Multilayer uniform circular arrays (UCAs) were predicted to generate dual-mode or multi-mode OAM beams. The advantages of planer structure and easy phase control lead to more attention on UCAs carrying OAM beams [17]–[20]. For example, in [18], a research on dual-OAM-mode antenna array was investigated, in which a UCA fed by two feeding networks was designed to generate $+1/-1$ OAM modes. In [13], a UCA using multi-layer structure was proposed to achieve $+/-1$ and $+/-2$ OAM beams, where the inner UCA and outer UCA produce different OAM beams with different modes independently. However, UCAs often suffer a complex feeding system, resulting in significant losses, low efficiency and high cost. Moreover, it is very challenging to design large OAM antenna arrays, as the feeding network is much more complicated than conventional antenna arrays due to the specific phase shift requirement [21]. Other types of antennas were also reported for OAM beam generation, such as travelling-wave ring-slot antenna [22], lens antenna [23], elliptical patch antenna and substrate integrated waveguide (SIW) antenna [24]. However, the drawbacks such as non-planar, high complexity and low efficiency still exist.

Transmitarray antennas (TAs) and reflectarray antennas (RAs) are an attractive alternative to lens antennas and the traditional phased array antennas because of their planar structure, low cost, simple feeding system and easy beam forming [25]–[29]. Using TAs or RAs is another way to generate OAM beams. The TAs or RAs consist of hundreds or thousands of periodic unit cells, which can be used to control the transmission phase or reflection phase to design a desired beam. The proposed unit cells are usually designed based on frequency selective surface (FSS), metasurface or microstrip antennas. In [30], a $+1$ mode OAM beam was produced by a transmitarray, which is constituted by the unit cell of split-ring FSS. In [31], a high efficiency folded reflectarray was designed for producing OAM beam. In mm-wave domain, an OAM transmitarray based on multi-layer phase-shifting surface was presented in [32]. Compared to UCAs, OAM beams produced by TAs or RAs have higher gain performance. However, one drawback of the most of reported transmitarray and reflecarray OAM antennas is that only one mode OAM beam can be produced, which is difficult to meet the dual-mode OAM beams requirement in future wireless communications. Although a generation method for dual-mode OAM beams was reported in [33], the different OAM beams were in different directions, which have many limits in wireless communications.

Inspired by TAs and dual-polarized antenna arrays, we propose a new strategy to realize a high-gain transmitarray generating dual-mode OAM beams in Ku band. This antenna can achieve multithread communication with a single transmitarray instead of two independent and orthogonal polarization OAM antennas for similar functions. In the proposed design, two compact dual-polarized wideband microstrip antennas are placed back-to-back as the unit cell. The approach for generating dual-mode OAM beams is explained. To verify the concept, a TA generating 0 mode OAM beam in x-polarization and $+1$ mode OAM beam in y-polarization is designed and fabricated. Excellent performance in terms of high gain, narrow divergence angle, low cost, planar structure is obtained. The experimental results agree well with the simulated ones, which show that the proposed transmitarray can produce 0 and $+1$ mode OAM beams successfully, with maximum gain of 26 dBi and 20 dBi, respectively. Meanwhile, a narrow divergence angle of $+/-5^{o}$ is obtained in $+1$ mode OAM beam.

II. TRANSMITARRAY DESIGN

The configuration of the proposed transmitarray is schematically shown in Fig. 1, which consists of two parts: feeding antenna and transmitarray. The transmitarray consists of receive-array, beam-forming structure and transmit-array,

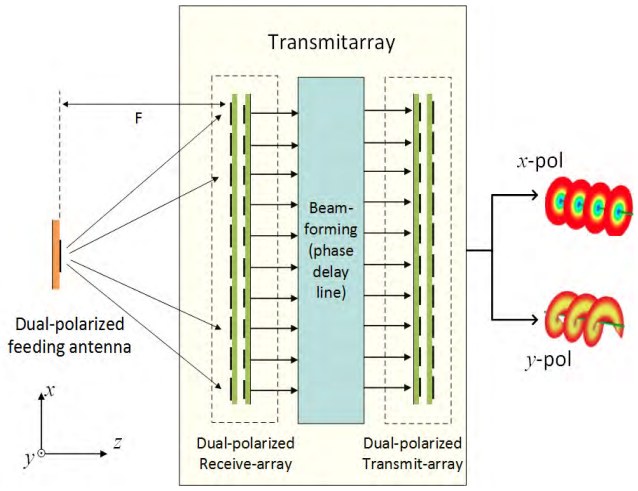

FIGURE 1. Scheme of transmitarray generating dual-mode OAM beams.

which is centrally illuminated by the incident waves from feeding antenna with the focal distance of F. The incident waves are received by receive-array and then transmitted by transmit-array. In the proposed design, the transmitarray operates in two orthogonal polarizations. Thus, the dual-mode OAM beams can be achieved in x- and y-polarizations, respectively.

A. DESIGN OF UNIT CELL

The unit cell of the proposed transmitarray is shown in Fig. 2, which is composed of two dual-polarized wideband microstrip antennas. The two antennas are placed back-to-back and share a common ground plane. The driven patch has two orthogonal feeding lines and is printed on the substrate of 0.5 mm Rogers 4003C (ε_r =3.55). To enhance the bandwidth, the parasitic patch, etched in 0.8 mm Rogers 4003C, is located above the driven patch with an air space of 1.5 mm. The size of driven patch and parasitic patch is 5 mm and 6.1 mm, respectively. Two metalized via holes surrounded by a circular disk etched in the ground plane are used to connect the feeding lines. The phase response can be adjusted by changing the lengths of the feeding lines.

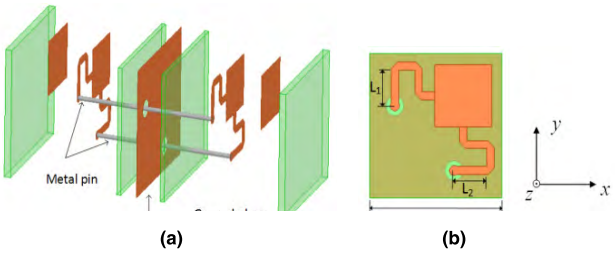

FIGURE 2. Unit cell: (a) 3-D exploded view; (b) top view of the unit cell.

To obtain dual-mode OAM beams, independent phase control in different polarization is necessary. This requirement can be regarded as that there is few interaction when the values of L_1 or L_2 vary uniquely. To verify this, the scatting response of the unit cell is investigated using CST Microwave Studio and the periodic boundary is considered during the simulation. Fig. 3 depicts the phase and magnitude of transmission coefficient versus different L_1 with fixed L_2 (4 mm). As can be seen, the proposed unit cell can get good transmission magnitude above −2 dB from 12.5 GHz to 15.2 GHz.

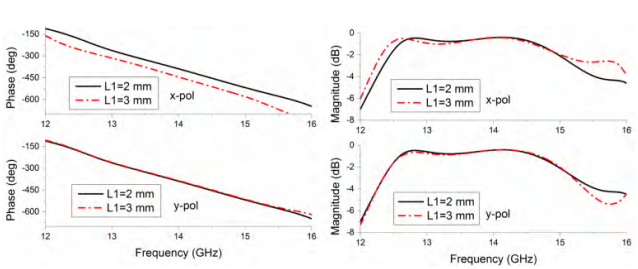

FIGURE 3. Phase and Magnitude of transmission coefficient in different L_1 with fixed L_2.

Meanwhile, there are few effects on the phase response in y-polarization when the feeding lines in x-polarization (L_1) varies. The simulated results show that the transmission phase can be controlled independently in each orthogonal polarization. Thus, it is feasible to produce dual-mode OAM beams in different polarizations.

Generally, the phase shift in a transmitarray should cover 360° with high transmission efficiency. Fig. 4 simulates the phase variation and magnitude in x-polarization. As can be seen, a full transmission phase range of 360° is achieved with well linearity at different frequencies. The transmission magnitude is better than −2 dB. The transmission phase curves at different frequencies are almost parallel to each other, which indicates the broadband performance of the unit cell. Due to similar structure and high isolation between x- and y-polarizations, it can be predicted that similar transmission coefficient in y-polarization can be obtained when L_2 is varied.

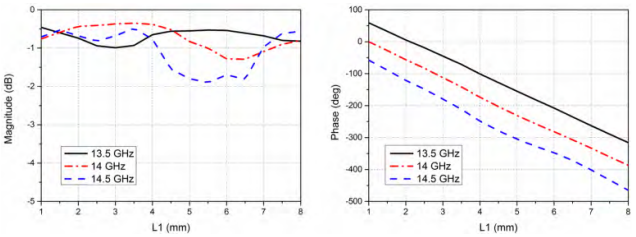

FIGURE 4. (a) The transmission magnitude of the unit cell at different frequencies; (b) the transmission phase of the unit cell at different frequencies.

In practice, most of the unit cells are not placed in the central area and they are illuminated by oblique incidences with different angles. It is necessary to analyze the performance of the unit cell under oblique incidence. Fig. 5 depicts the transmission phase and magnitude at different oblique incidence angles. From the simulated results, within 40° oblique incidence, the transmission magnitude can keep higher than −2 dB with small variation of transmission phase. According to the simulated results, it can be concluded that the proposed unit cell has low transmission loss and less sensitivity to the

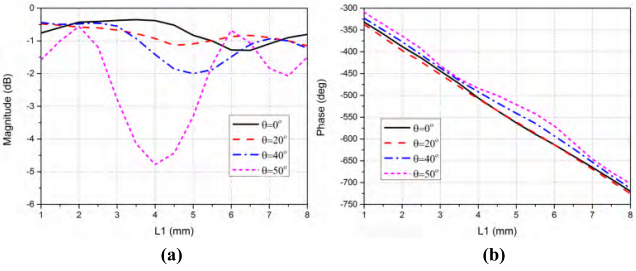

FIGURE 5. (a) the transmission magnitude of the unit cell with different oblique incidence; (b) the transmission phase of the unit cell with different oblique incidence.

oblique incident electric field, which is desired to constitute a transmisstarray.

B. DESIGN METHOD OF DUAL-MODE OAM BEAMS

The process for generating OAM beams using transmitarray can be divided into two steps: the first step is phase compensation. This step coverts the spherical phase front from the feeding antenna to planar phase front. The second step is phase superposition, which means add a spiral phase on the converted planar phase front. The spiral phase imposes a total phase shift of $2\pi l$ around one azimuthal cycle according to the OAM mode l.

The phase distribution of the first step is defined as $\varphi_{ij(p)}$, which can be obtained according to the following function

$$\varphi_{ij(p)} = k_0 \times \sqrt{(x_i - x_f)^2 + (y_j - y_f)^2 + z_f^2} \tag{1}$$

where $(x_i\ ,\ y_j)$ is the position of unit cell and $(x_f,\ y_f,\ z_f)$ is the position of the feeding antenna. Here, we assume the transmitarray is placed at the plane of z =0, namely xoy plane.

The spiral phase plane can be obtained based on the function (2)

$$\varphi_{\text{spp}} = l \times \varphi = l \times \arctan(x_i/y_j) \tag{2}$$

where l is the OAM mode. Thus, the final phase distribution for generating OAM beams can be concluded as the following function

$$\varphi_{ij(\text{OAM})} = \varphi_{ij(p)} + \varphi_{\text{spp}} \tag{3}$$

In the proposed transmitarray, 0 mode and +1 mode are selected to verify the design concept. Based on the discussion, a square-aperture transmitarray consisting of 14×14 unit cells is built. A dual-polarized wideband microstrip antenna, which is similar to the unit cell, is used as the feeding antenna. Considering the aperture size of the transmitarry and radiation pattern of the feed antenna, the focal-length is optimized as 113 mm. According to function (1), (2) and (3), the phase distributions for generating 0 mode and +1 mode OAM beams are calculated and shown in Fig. 6(a) and Fig. 6(b), respectively. As can be seen, the phase distribution of 0 OAM mode is symmetric to the array center, which is plane wave phase distribution actually. The phase distribution of +1 mode OAM beam shows a 360° clockwise phase shift.

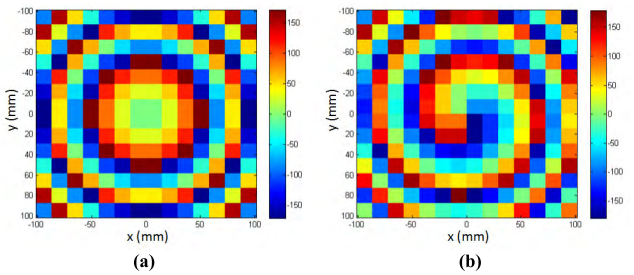

FIGURE 6. The phase distributions: (a) 0 OAM mode; (b) +1 OAM mode.

III. SIMULATION AND ANALYSIS

The proposed transmitarray is constituted based on the calculated phase distributions. Fig. 7 shows the geometry of the transmitarray. In the design, the phase delay lines in x-polarization (L_1) are employed to produce 0 mode OAM beam and the phase delay lines (L_2) in y-polarization are used to generate +1 mode OAM beam. Full-wave simulation using commercial software HFSS is carried out.

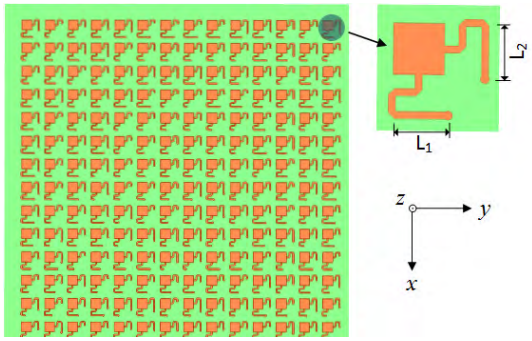

FIGURE 7. The geometry of the proposed transmitarray.

The simulated radiation patterns are shown in Fig. 8. The 0 mode and +1 mode OAM beams are produced successfully as expectation. Due to large aperture, high transmission coefficient and accurate phase compensation, the radiation patterns have high gain performance. At 13.5 GHz, the simulated gain reaches 25.6 dBi in 0 OAM mode and 19.9 dBi in +1 OAM mode, respectively.

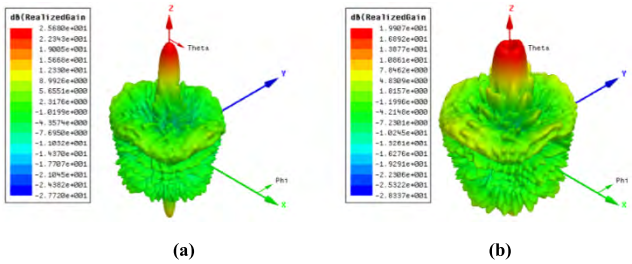

FIGURE 8. The simulated radiation patterns at 13.5 GHz: (a) 0 mode OAM beam; (b) +1 mode OAM beam.

A small divergence angle of +/−5° in +1 mode OAM beam is achieved. Compared to conventional UCAs for generating OAM beams, the divergence angle in this proposed antenna has a dramatic improvement, which can be used to increase the OAM-based communication link distance. To further demonstrate the principle of generating OAM beams, the side view of E-field is present in Fig. 9. As can be seen, the electromagnetic waves produced by the feeding antenna is reconstructed when it spreads through the transmitarray. It is observed that the incident x- and y-polarized spherical waves from the feeding antenna is transformed to 0 mode OAM beam and +1 mode OAM beam, respectively.

For +1 mode OAM beam, there is an amplitude null in the center of radiation patterns. This null area becomes larger

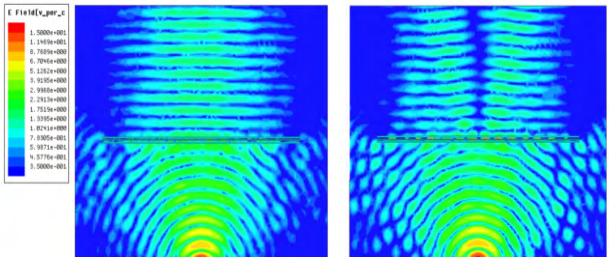

FIGURE 9. The side view of E-fields: (a) x-polarization; (b) y-polarization.

with the increase of propagation distance, which makes challenge in long-distance OAM-based communication. To study the stability of the +1 mode OAM beam, the evolution processes is simulated and shown in Fig. 10. In this simulation, a reference plane with $500\times500\text{mm}^2$ is mounted above the proposed transmitarray as reference plane. The distance between the reference plane and the transmitarray is selected as 220 mm (≈10 λ at 13.5 GHz), 330 mm (≈15 λ at 13.5 GHz), 440 mm (≈20 λ at 13.5 GHz) and 520 mm (≈23 λ at 13.5 GHz), respectively. For content concise, the simulated phase fronts and E-field intensity at the distance of 330 mm and 520 mm are plotted in Fig. 10. As can be seen, the properties of +1 mode OAM beam, such as spatial phase distribution and ring-shaped amplitude intensity, still keep very well even when the OAM beam propagates to a long distance. Conclusively, the +1 mode OAM beam has a good stable performance.

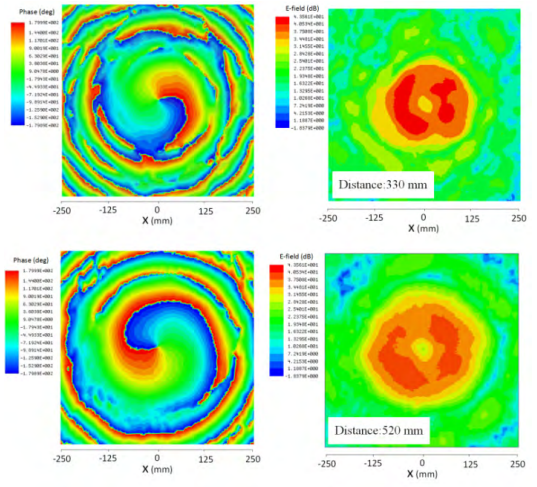

FIGURE 10. Simulated phase fronts and E-field intensity of the +1 mode OAM beam with different distance.

IV. FABRICATION AND MEASUREMENT

To verify the design, a prototype is fabricated, assembled and measured, as shown in Fig. 11. The overall dimension of the proposed transmittarry is 240×240 mm^2 with effective area of 203×203 mm^2, which is covered by 14×14 unit cells. To support the whole array and create air space, several nylon spacers are employed between every two substrate layers. These nylon spacers are considered during the simulation.

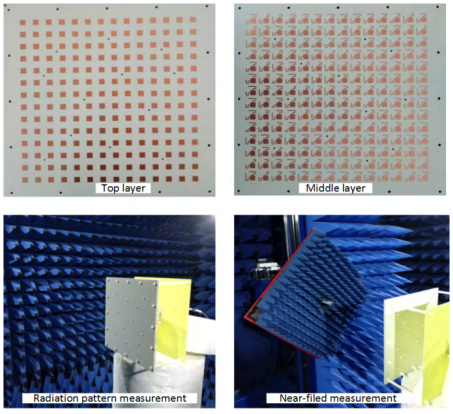

FIGURE 11. The antenna prototype and antenna measurement in anechoic chamber.

A. RADIATION PATTERNS

The measured and simulated radiation patterns of dual-mode OAM beams at different frequencies are plotted in Fig. 12 and Fig. 13, respectively. The both of 0 mode and +1 mode OAM beams are well produced by the proposed antenna. Good agreement is achieved between numerical calculation and measurement. Within the frequency range from 13 GHz to 15GHz, the measured gain of 0 mode OAM beams is above 20 dBi with maximum gain of 26 dBi at 13.8 GHz. At the

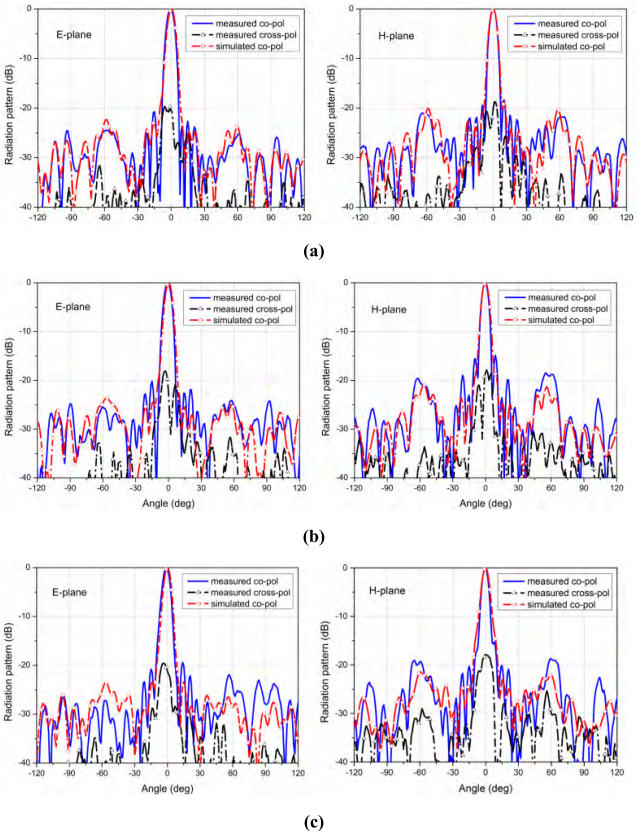

FIGURE 12. The measured 0 mode OAM beams: (a) 13 GHz; (b)13.5 GHz; (c) 14 GHz.

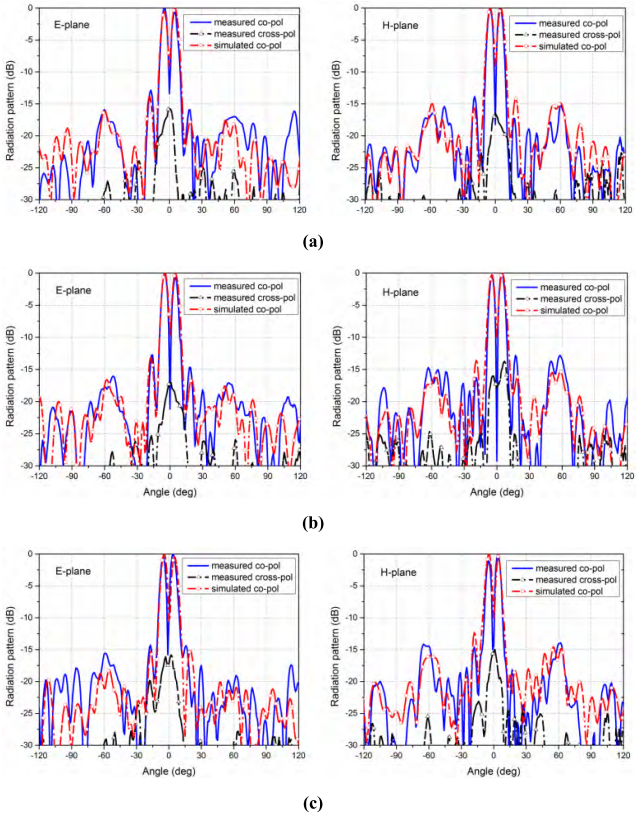

FIGURE 13. The measured +1 mode OAM beams: (a) 13 GHz; (b) 13.5 GHz; (c) 14 GHz.

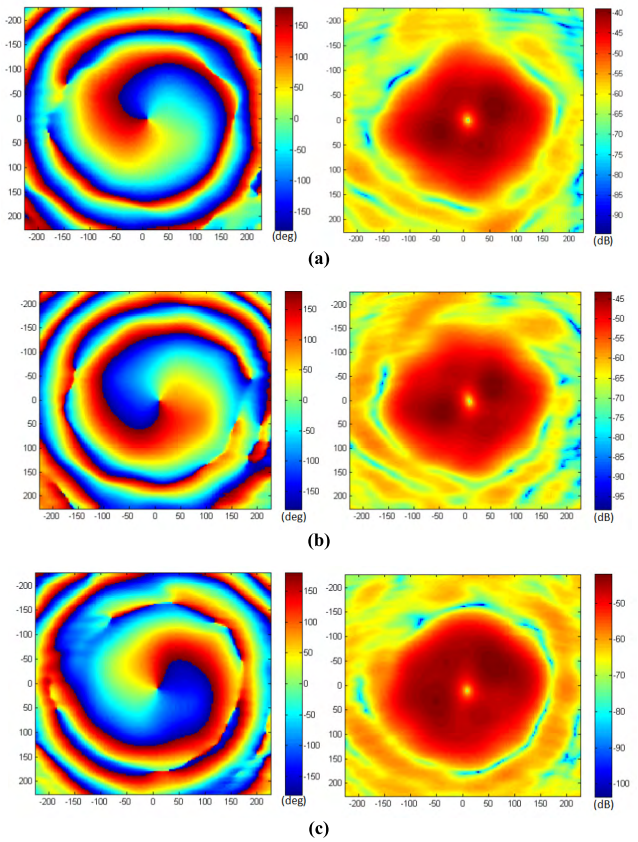

FIGURE 14. The measured near-field radiation patterns of the produced +1 mode OAM beams at different frequencies: (a) 13 GHz; (b)13.5 GHz; (c) 14 GHz.

same frequency range, the measured gain of +1 mode OAM beams is above 14.2 dBi with maximum gain of 20 dBi at 13.6 GHz. The 3-dB beam width in 0 mode OAM beam is around 6.5°. The maximum side lobe level (SLL) is less than −14 dB and the cross-polarization level less than −15 dB, respectively. The measured divergence angle of the +1 mode OAM beams is approximately +/−5°.

B. PHASE FRONTS AND E-FIELD INTENSITY

The phase fronts and E-field intensity of +1 mode OAM beams are measured using near field measure system. The scanning plane in the near-field measure system is set as 520×520 mm^2 with the measure step of 3mm. The distance between the scanning plane and the transmitarray is 530 mm. As shown in Fig. 14, the phase fronts of the +1 mode OAM beam can be generated with continuously distributed spatial phase. Meanwhile, the measured E-field intensity has a deep null in the center of scanning plane. It can be indicated that the designed transmittarray can produce good +1 mode OAM beams.

C. PERFORMANCE COMPARISON

Table 1 compares the proposed transmitarray with other reported antennas carrying OAM beams. This comparison

TABLE 1. Comparison with other reported OAM antennas.

Ref.	Antenna type	Planar structure	Feeding network	OAM mode	Gain (dBi)
[17]	Uniform circular array	Yes	Complex	+1	Not given
[18]	Bow-tie dipole array	Yes	Complex	±1	Not given
[20]	Reconfigurable Patch Array	Yes	Complex	±1	5.9
[22]	Ring-slot with parabolic reflector	No	No need	±2/±3	21.9
[31]	Folded reflectarray	Yes	No need	+1	21.5
[32]	Flat-lens	Yes	No need	+1	21.5
This work	Transmitarray	Yes	No need	0 /+1	26 /20

mainly focuses on antenna type, planar structure, feeding network, OAM modes and antenna gain. The comparison shows that using array antennas can simply achieve dual-mode OAM beams. But the feeding network is complex. Most of the reflectarrays or transmitarrays can achieve OAM waves with only one mode. As comparison, the proposed antenna has the advantages of planar structure, no need of feeding network, dual-mode OAM beams and high gain. It is worth pointing out that although the present design in this paper is generating 0 and +1 mode OAM beams, the design method is also adapted to other two types of beams.

V. CONCLUSION

A novel Ku-band high-gain transmitarray antenna for generating dual-mode OAM beams is presented and studied in this paper. The phase delay lines connecting the receive-array and transmit-array are employed to cover the required phase variation. The design approach for producing the two types of beams is analyzed. The stability of the generated +1 mode OAM beam is discussed. Both the full-wave simulation and the prototype measurement validate the design approach successfully. The 0 mode and +1 mode OAM beams are obtained simultaneously. The measured maximum gain reaches 26 dBi in 0 mode OAM beam and 20 dBi in +1 mode OAM beam, respectively. The divergence angle of +1 mode OAM beam is only $+/-5^{o}$. This proposed transmitarray can be a promising candidate in future high capacity communications.

REFERENCES

[1] S. M. Mohammadi *et al.*, "Orbital angular momentum in radio—A system study," *IEEE Trans. Antennas Propag.*, vol. 58, no. 2, pp. 565–572, Feb. 2010.

[2] Z. Zhang *et al.*, "An orbital angular momentum-based in-band full-duplex communication system and its mode selection," *IEEE Commun. Lett.*, vol. 21, no. 5, pp. 1183–1186, May 2017.

[3] M. W. Beijersbergen *et al.*, "Multiphoton resonances and Bloch-Siegert shifts observed in a classical two-level system," *Phys. Rev. A, Gen. Phys.*, vol. 45, no. 3, pp. 1810–1815, 1992.

[4] H. Zhou, J. Dong, S. Yan, Y. Zhou, L. Shi, and X. Zhang, "Manipulation of orbital angular momentum beams based on space diffraction compensation," *Opt. Express*, vol. 22, no. 15, pp. 17756–17761, 2014.

[5] M. Chen, M. Mazilu, Y. Arita, E. M. Wright, and K. Dholakia, "Optical trapping with a perfect vortex beam," *Proc. SPIE*, vol. 9164, p. 91640K, Sep. 2014.

[6] V. V. Kotlyar, A. A. Kovalev, and A. P. Porfirev, "An optical tweezer in asymmetrical vortex bessel-Gaussian beams," *J. Appl. Phys.*, vol. 120, no. 6, p. 023101, 2016.

[7] Y. Yue *et al.*, "Mode properties and propagation effects of optical orbital angular momentum (OAM) modes in a ring fiber," *IEEE Photon. J.*, vol. 4, no. 2, pp. 535–543, Apr. 2012.

[8] J. Wang *et al.*, "Terabit free-space data transmission employing orbital angular momentum multiplexing," *Nature Photon.*, vol. 6, pp. 488–496, Jun. 2012.

[9] B. Thidé *et al.*, "Utilization of photon orbital angular momentum in the low-frequency radio domain," *Phys. Rev. Lett.*, vol. 99, no. 8, p. 087701, Aug. 2007.

[10] F. Tamburini *et al.*, "Experimental verification of photon angular momentum and vorticity with radio techniques," *Appl. Phys. Lett.*, vol. 99, no. 20, p. 204102, 2011.

[11] F. Tamburini, E. Mari, A. Sponselli, B. Thidé, A. Bianchini, and F. Romanato, "Encoding many channels on the same frequency through radio vorticity: First experimental test," *New J. Phys.*, vol. 14, no. 11, pp. 78001–78004, 2012.

[12] Y. Yan *et al.*, "High-capacity millimetre-wave communications with orbital angular momentum multiplexing," *Nature Commun.*, vol. 5, p. 4876, Mar. 2014.

[13] Z. Zhao *et al.*, "A dual-channel 60 GHz communications link using patch antenna arrays to generate data-carrying orbital-angular-momentum beams," in *Proc. IEEE Int. Conf. Commun.* May 2016, pp. 1–6.

[14] A. Bennis, R. Niemiec, C. Brousseau, K. Mahdjoubi, and O. Emile, "Flat plate for OAM generation in the millimeter band," in *Proc. Eur. Conf. Antennas Propag. (EuCAP)*, Gothenburg, Sweden, Apr. 2013, pp. 3203–3207.

[15] L. Cheng, W. Hong, and Z.-C. Hao, "Generation of electromagnetic waves with arbitrary orbital angular momentum modes," *Sci. Rep.*, vol. 4, Apr. 2014, Art. no. 4814.

[16] G. A. Turnbull, D. A. Robertson, G. M. Smith, L. Allen, and M. J. Padgett, "The generation of free-space Laguerre-Gaussian modes at millimetre-wave frequencies by use of a spiral phaseplate," *Opt. Commun.*, vol. 127, nos. 4–6, pp. 183–188, 1996.

[17] Q. Bai, A. Tennant, and B. Allen, "Experimental circular phased array for generating OAM radio beams," *Electron. Lett.*, vol. 50, no. 20, pp. 1414–1416, Sep. 2014.

[18] B. Liu, Y. Cui, and R. Li, "A broadband dual-polarized dual-OAM-mode antenna array for OAM communication," *IEEE Antennas Wireless Propag. Lett.*, vol. 16, pp. 744–747, 2017.

[19] W. Zhang *et al.*, "Mode division multiplexing communication using microwave orbital angular momentum: An experimental study," *IEEE Trans. Wireless Commun.*, vol. 16, no. 2, pp. 1308–1318, Feb. 2017.

[20] Q. Liu, Z. N. Chen, Y. Liu, F. Li, Y. Chen, and Z. Mo, "Circular polarization and mode reconfigurable wideband orbital angular momentum patch array antenna," *IEEE Trans. Antennas Propag.*, vol. 66, no. 4, pp. 1796–1804, Apr. 2018.

[21] F. Qin *et al.*, "A simple low-cost shared-aperture dual-band dual-polarized high-gain antenna for synthetic aperture radars," *IEEE Trans. Antennas Propag.*, vol. 64, no. 7, pp. 2914–2922, Jul. 2016.

[22] W. Zhang, "Four-OAM-mode antenna with traveling-wave ring-slot structure," *IEEE Antennas Wireless Propag. Lett.*, vol. 16, pp. 194–197, 2017.

[23] X. Bai, X. Liang, R. Jin, J. Geng, "Generation of OAM radio waves with three polarizations using circular horn antenna array," in *Proc. Eur. Conf. Antennas Propag. (EuCAP)*, Apr. 2015, pp. 1–4.

[24] Y. Chen, S. Zheng, H. Chi, X. Jin, and X. Zhang, "Half-mode substrate integrated waveguide antenna for generating multiple orbital angular momentum modes," *Electron. Lett.*, vol. 52, no. 9, pp. 684–686, Apr. 2016.

[25] J. R. Reis, R. F. S. Caldeirinha, A. Hammoudeh, and N. Copner, "Electronically reconfigurable FSS-inspired transmitarray for 2-D beamsteering," *IEEE Trans. Antennas Propag.*, vol. 65, no. 9, pp. 4880–4885, Sep. 2017.

[26] R. Y. Wu, Y. B. Li, W. Wu, C. B. Shi, and T. J. Cui, "High-gain dual-band transmitarray," *IEEE Trans. Antennas Propag.*, vol. 65, no. 7, pp. 3481–3488, Jul. 2017.

[27] H. X. Xu, T. Cai, Y.-Q. Zhuang, Q. Peng, G.-M. Wang, and J.-G. Liang, "Dual-mode transmissive metasurface and its applications in multi-beam transmitarray," *IEEE Trans. Antennas Propag.*, vol. 65, no. 4, pp. 1797–1806, Apr. 2017.

[28] C. Jouanlanne *et al.*, "Wideband linearly polarized transmitarray antenna for 60 GHz backhauling," *IEEE Trans. Antennas Propag.*, vol. 65, no. 3, pp. 1440–1445, Mar. 2017.

[29] L. Di Palma, A. Clemente, L. Dussopt, R. Sauleau, P. Potier, and P. Pouliguen, "Circularly polarized transmitarray with sequential rotation in Ka-band," *IEEE Trans. Antennas Propag.*, vol. 63, no. 11, pp. 5118–5124, Nov. 2015.

[30] D. Zelenchuk and V. Fusco, "Split-ring FSS spiral phase plate," *IEEE Antennas Wireless Propag. Lett.*, vol. 12, pp. 284–287, 2013.

[31] X. Y. Lei and Y. J. Cheng, "High-efficiency and high-polarization separation reflectarray element for OAM-folded antenna application," *IEEE Antennas Wireless Propag. Lett.*, vol. 16, pp. 1357–1360, 2017.

[32] Y. Chen *et al.*, "A flat-lensed spiral phase plate based on phase-shifting surface for generation of millimeter-wave OAM beam," *IEEE Antennas Wireless Propag. Lett.*, vol. 15, pp. 1156–1358, 2016.

[33] S. Yu *et al.*, "Generating multiple orbital angular momentum vortex beams using a metasurface in radio frequency domain," *Appl. Phys. Lett.*, vol. 108, no. 24, p. 241901, 2016.

[34] J. U. Duncombe, "Infrared navigation—Part I: An assessment of feasibility," *IEEE Trans. Electron Devices*, vol. ED-11, no. 1, pp. 34–39, Jan. 1959, doi: 10.1109/TED.2016.2628402.

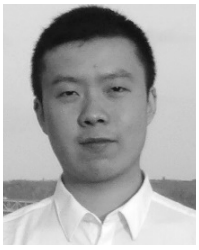

FAN QIN received the B.S. degree in electronic and information engineering and the M.S. degree in electromagnetic field and the Ph.D. degree in electromagnetic wave and microwave technology from Northwestern Polytechnical University, Xi'an, China, in 2010 and 2016, respectively. He is currently a Lecturer with the State Key Laboratory of Integrated Services Networks, Xidian University. His research interests include OAM antenna design, circularly polarized antennas, dual-band/multiband antenna arrays, meta materials antennas, and transmit arrays.

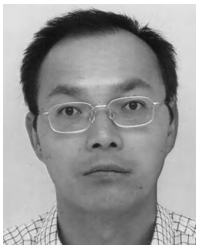

STEVEN GAO received the Ph.D. degree in microwave engineering from Shanghai University, Shanghai, China, in 1999. He is currently a Professor and the Chair of RF and microwave engineering with the University of Kent, Canterbury, U.K. He has authored over 250 papers and co-authored two books, including the *Space Antenna Handbook* (Wiley, 2012) and the *Circularly Polarized Antennas* (IEEE-Wiley, 2014). He holds several patents in smart antennas and RF. His current research interests include smart antennas, phased arrays, satellite antennas, RF/microwave/millimeter-wave/terahertz circuits, satellite communications, ultra-wideband radars, synthetic-aperture radars, and mobile communications.

WEN-CHI CHENG (M'14–SM'18) received the B.S. and Ph.D. degrees in telecommunication engineering from Xidian University, China, in 2008 and 2014, respectively. He joined the Department of Telecommunication Engineering, Xidian University, in 2013, as an Assistant Professor, where he is currently an Associate Professor. He has authored over 50 international journal and conference papers in the IEEE JOURNAL ON SELECTED AREAS IN COMMUNICATIONS, the *IEEE Magazines*, the IEEE TRANSACTIONS, the IEEE INFOCOM, GLOBECOM, and ICC. His current research interests include 5G wireless networks and orbital-angular-momentum-based wireless communications. He received the Young Elite Scientist Award of CAST, the Best Dissertation (Rank 1) of the China Institute of Communications, the Best Paper Nomination for the IEEE GLOBECOM 2014, and the Outstanding Contribution Award for Xidian University. He has served or serving as the Publicity Chair for ICC 2019 and a TPC Member for the IEEE INFOCOM, GLOBECOM, and ICC. He has served or serving as an Associate Editor for the IEEE ACCESS.

YI LIU (M'09–SM'17) received the B.S. degree from Dalian Jiaotong University, Dalian, China, in 2002, and the M.S. and Ph.D. degrees from Xidian University, Xi'an, China, in 2005, and 2007, respectively, all in communication engineering. Since 2008, he has been with the State Key Laboratory of Integrated Service Network, Xidian University, where he is currently a Professor. From 2011 to 2012, he was a Visiting Scholar with the University of Delaware, Newark, DE, USA. His research interests include signal processing for wireless communications, MIMO and OFDM wireless communications, and cooperative communications

HAI-LIN ZHANG (M'97) received the B.S. and M.S. degrees from Northwestern Polytechnic University, Xi'an, China, in 1985 and 1988, respectively, and the Ph.D. degree from Xidian University, Xi'an, in 1991. In 1991, he joined the School of Telecommunications Engineering, Xidian University, where he is currently a Senior Professor and the Dean. He is also the Director of the Key Laboratory in Wireless Communications sponsored by the China Ministry of Information Technology, a Key Member of the State Key Laboratory of Integrated Services Networks, one of the state government specially compensated scientists and engineers, a field leader in telecommunications and information systems with Xidian University, an Associate Director of the National 111 Project. He has authored over 150 papers in journals and conferences. His current research interests include key transmission technologies and standards on broadband wireless communications for 5G and 5G-beyond wireless access systems.

GAO WEI was born in Xi'an, Shaanxi, China, in 1963. He received the Ph.D. degree from Northwestern Polytechnical University, Xi'an, China, in 2008. He is currently a Professor at the School of Electronics and Information, Northwestern Polytechnical University. His research interests include antenna design, microwave measurement, and microwave communication.